

Cationic Motions and Order–Disorder Phase Transitions in Layer Crystals with a Rotator Phase, $(n\text{-C}_5\text{H}_{11}\text{NH}_3)_2\text{ZnCl}_4$ and $(n\text{-C}_{12}\text{H}_{25}\text{NH}_3)_2\text{ZnCl}_4$

Keizo Horiuchi,* Himiko Takayama,[†] Shin'ichi Ishimaru,[†] and Ryuichi Ikeda[†]

Faculty of Science, University of the Ryukyus, Nishihara-cho, Okinawa 903-0213

[†]Department of Chemistry, University of Tsukuba, Tsukuba 305-0006

(Received August 26, 1999)

¹H NMR spin-lattice relaxation times T_1 and $T_{1\rho}$ as well as the electrical conductivity were measured as a function of temperature in $(n\text{-C}_5\text{H}_{11}\text{NH}_3)_2\text{ZnCl}_4$ and $(n\text{-C}_{12}\text{H}_{25}\text{NH}_3)_2\text{ZnCl}_4$. The highest-temperature solid phase in both compounds was found to be the rotator phase, where rod-like cations perform uniaxial reorientations about the molecular long axes accompanied by conformational disordering and translational self-diffusion of the cations within the layer perpendicular to c -axis. In the rotator phase, the cations are considered to have a non-intercalated double layer structure. These rotator phases were shown to be quite analogous to those reported in n -alkylammonium chlorides. $(n\text{-C}_5\text{H}_{11}\text{NH}_3)_2\text{ZnCl}_4$ undergoes four structural phase transitions, while $(n\text{-C}_{12}\text{H}_{25}\text{NH}_3)_2\text{ZnCl}_4$ exhibits a single transition above ca. 120 K. All of these transitions were shown to be of order–disorder type.

The rotator phase was first found in solid n -paraffins where the constituent molecules adopt dynamically disordered orientations about their molecular long axes.¹ The molecular motions in this phase, however, could not be fully determined because this phase is formed in a narrow temperature range of less than 10 K. Recently, we discovered a quite analogous phase in n -alkylammonium chlorides $\text{C}_n\text{H}_{2n+1}\text{NH}_3\text{Cl}$ ($n = 3\text{--}10, 12$) over a quite wide temperature range of more than 100 K.^{2–6} The crystal structure of this rotator phase is tetragonal (space group $P4/nmm$) with a lamellar-type double-layered structure. A new characteristic molecular motion found in this phase in addition to the uniaxial rotation of alkylammonium chains, is two-dimensional translational self-diffusion in the lamellar plane perpendicular to the molecular long axis. By comparison with the plastic crystal where the three-dimensional rotation and diffusion of constituent globular molecules or ions take place,⁷ we can name the rotator phase “a low-dimensional plastic crystal” because of the restricted motions such as 1D rotation and 2D diffusion. Thermal measurements also suggest that the rotator phase is a highly disordered crystalline state similar to the plastic crystal; the melting entropies ΔS_m observed in the n -alkylammonium chlorides are smaller than $20 \text{ J K}^{-1} \text{ mol}^{-1}$,^{2–6} reported as one of the conditions for the formation of the plastic crystal.⁷ At the same time, we note that this highly anisotropic crystalline state of lamellar-type double layer structure resembles the smectic liquid crystal, although the centers of gravity of constituent molecules in the layer are disordered in the liquid crystal.

Our present interest is to find rotator phases in systems different from n -alkylammonium chlorides. Recently, we have found the rotator phase in di- n -alkylammonium bromides

$(\text{C}_n\text{H}_{2n+1})_2\text{NH}_2\text{Br}$ ($n = 2\text{--}4$),⁸ which has a crystal structure of $I4/mmm$ analogous to that of $P4/nmm$. Di- n -alkylammonium tetrahalogenozincates $(n\text{-C}_n\text{H}_{2n+1}\text{NH}_3)_2\text{ZnX}_4$ ($X = \text{Cl}, \text{Br}$) are known to belong to the $A_2\text{BX}_4$ family with the $\beta\text{-K}_2\text{SO}_4$ structure (space group $Pnma$),^{9,10} and we have already studied some short-chain compounds of them with a prime interest in their structural phase transitions.^{11–14} The crystal structures in these compounds are characterized by a triple-layered structure that consists of two-dimensional layers made by isolated BX_4 ions being sandwiched by layers of alkylammonium ions. The title compounds, $(n\text{-C}_5\text{H}_{11}\text{NH}_3)_2\text{ZnCl}_4$ and $(n\text{-C}_{12}\text{H}_{25}\text{NH}_3)_2\text{ZnCl}_4$, have been reported to have ΔS_m smaller than $20 \text{ J K}^{-1} \text{ mol}^{-1}$.¹⁵ From these facts, we may expect the title compounds to have rotator phases. In the present study, the cationic dynamics and structural phase transitions were investigated by the measurements of the temperature dependence of ¹H NMR relaxation times and the electrical conductivity.

Experimental

$(n\text{-C}_5\text{H}_{11}\text{NH}_3)_2\text{ZnCl}_4$ and $(n\text{-C}_{12}\text{H}_{25}\text{NH}_3)_2\text{ZnCl}_4$ prepared by the methods described in Ref. 15 were identified by X-ray and thermal measurements as well as by chemical analyses. Anal. Calcd for $(n\text{-C}_5\text{H}_{11}\text{NH}_3)_2\text{ZnCl}_4$: C, 31.31; H, 7.36; N, 7.31%. Found: C, 31.31; H, 7.51; N, 7.19%. Calcd. for $(n\text{-C}_{12}\text{H}_{25}\text{NH}_3)_2\text{ZnCl}_4$: C, 49.70; H, 9.75; N, 4.83%. Found: C, 49.84; H, 9.94; N, 4.83%. X-Ray powder diffraction was measured using $\text{Cu K}\alpha$ radiation with a Philips X'Pert-MPD and a Rigaku RINT-1500 diffractometer for $(n\text{-C}_5\text{H}_{11}\text{NH}_3)_2\text{ZnCl}_4$ and $(n\text{-C}_{12}\text{H}_{25}\text{NH}_3)_2\text{ZnCl}_4$, respectively. Differential scanning calorimetry (DSC) was carried out with a DSC120 calorimeter from Seiko Instruments Inc. DTA was also performed on $(n\text{-C}_{12}\text{H}_{25}\text{NH}_3)_2\text{ZnCl}_4$ using a home-made apparatus¹⁶ over the range 300–480 K. The sample temperatures

in DTA and the following measurements were determined using chromel–constantan thermocouples within ± 1 K.

The ^1H NMR spin-lattice relaxation time, T_1 , was measured by a Bruker SXP-100 spectrometer at Larmor frequency of 40 MHz and by a home-made pulsed spectrometer¹⁷ at frequencies of 10–25 MHz. T_1 was determined by a 180° - τ - 90° pulse sequence. The ^1H NMR spin-lattice relaxation time in the rotating frame, $T_{1\rho}$, and the second moment, M_2 , of the resonance linewidth were measured with a Bruker SXP-100 spectrometer at a Larmor frequency of 40 MHz using the spin-locking method¹⁸ applying an r.f. magnetic field of 3.97 G and the solid-echo method¹⁹ with a 90°_x - τ - 90°_y pulse sequence, respectively.

The temperature dependence of electrical conductivity was measured at 1 kHz by the two-terminal method with a home-made apparatus using a Yokogawa Hewlett–Packard 4261A LCR meter. The powdered sample was pressed into a disc of 10 mm in diameter and ca. 1 mm thick, and mounted on Cu electrodes using graphite electrodes (Acheson Electrodegraph 199).

Results and Analysis

(*n*-C₅H₁₁NH₃)₂ZnCl₄. In our thermal measurements, (*n*-C₅H₁₁NH₃)₂ZnCl₄ showed four first-order structural phase transitions at 141.5, 148, 250, and 349 K, in agreement with the reported results.²⁰ These five solid phases are named as I, II, III, IV, and V in the order of decreasing temperature. Crystal structures in phases I, II, and III were reported to be all orthorhombic, their space groups being *Pnma* for II and *P2₁2₁2₁* for III.^{10,20} X-Ray powder diffraction patterns taken at 293 ± 1 K in phase II and at 390 ± 2 K in phase I were well explained using the reported lattice parameters.^{10,20}

Temperature dependences of ^1H NMR T_1 measured at 40.1 and 10.8 MHz are shown in Fig. 1. A discontinuity in T_1 was observed only at the I–II transition, although four phase transitions are first-order. The observed T_1 curve gave a minimum around 150 K and a Larmor-frequency dependence only on the low-temperature side of T_1 minimum. This temperature dependence is attributable to the magnetic dipolar relaxation caused by thermal molecular motions, and can be analyzed by the BPP equation²¹ using the Arrhenius relationship between the motional correlation time, τ_c , and the motional activation energy, E_a , as given by

$$\tau_c = \tau_{c0} \exp\left(\frac{E_a}{RT}\right). \quad (1)$$

The obtained best fit T_1 curves are displayed in Fig. 1 and the determined values of motional parameters are listed in Table 1. The assignment of motional modes was carried out by calculating M_2 values.²² Since proton positions are unavailable on the crystal structure data, the calculation was performed by assuming proton positions using a standard value for an alkylammonium ion.

The T_1 maximum observed in the high-temperature range of phase II suggests the onset of a new motion other than the NH_3^+ rotation. We assigned it to the 180° flip of the whole cations about the molecular long axes, because in short alkyl chain salts such as *n*-C₄H₉NH₃X (X = Cl, Br, I)^{3,23,24} and *n*-C₅H₁₁NH₃Cl,⁴ the 180° -flip or analogous two-site jumps

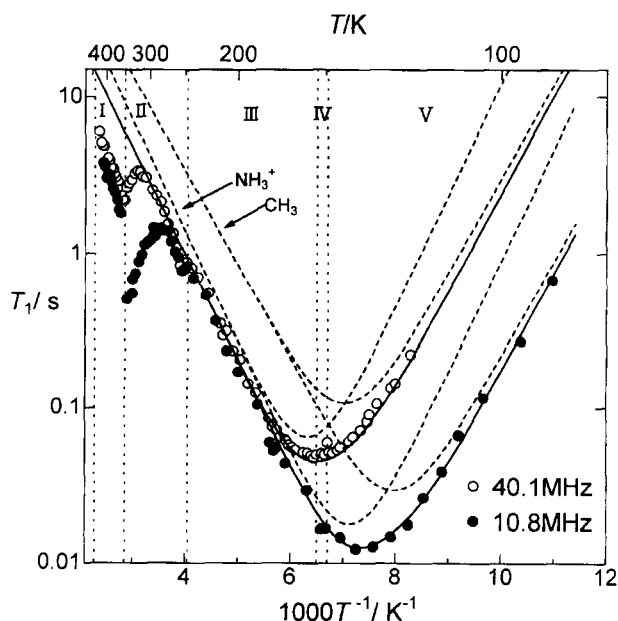


Fig. 1. Temperature dependences of ^1H NMR T_1 observed in (*n*-C₅H₁₁NH₃)₂ZnCl₄. Solid curves are the best-fitted calculated ones. Broken curves are contributions from respective molecular motions (see text). Dotted lines represent the phase transition temperatures.

Table 1. Activation Energies, E_a , Pre-exponential Factors, τ_{c0} , and Motional Modes of *n*-Pentylammonium Cations in (*n*-C₅H₁₁NH₃)₂ZnCl₄ Determined by ^1H NMR T_1 and $T_{1\rho}$

Phase	E_a	τ_{c0}	Motional mode
	kJ mol^{-1}	10^{-12} s	
III–V	12 ± 1	14 ± 1	CH_3 rotation
	14 ± 1	0.73 ± 0.07	NH_3^+ rotation
II	34 ± 3		180° flip
I	18 ± 2		Axial rotation + conformational disorder
	72 ± 7		Self-diffusion
	$85 \pm 9^{\text{a}}$		Self-diffusion

a) Derived from electrical conductivity.

of the entire alkyl chain were found in the low-temperature phases. We therefore analysed the T_1 variations in phase II by a superimpose of 180° -flip and NH_3^+ rotation, giving the best fitted curves displayed in Fig. 2.

^1H NMR $T_{1\rho}$ observed in phase I is shown in Fig. 3 along with T_1 data. The increase in T_1 and the decrease in $T_{1\rho}$ with increasing temperature suggest that two different molecular motions are effective in the relaxation process in this phase: one is rapid and the other is slow. The temperature dependence of M_2 in the range 308–411 K is represented in Fig. 4. M_2 values in phase I were abruptly reduced to less than 2 G^2 from ca. 20 G^2 just below the transition temperature in phase II, implying the onset of a new motion in phase I that averages most of the proton dipolar interactions. It is the rapid motion that is responsible for this large M_2 reduction, and the motion is considered to be the axial rotation of rigid cations about

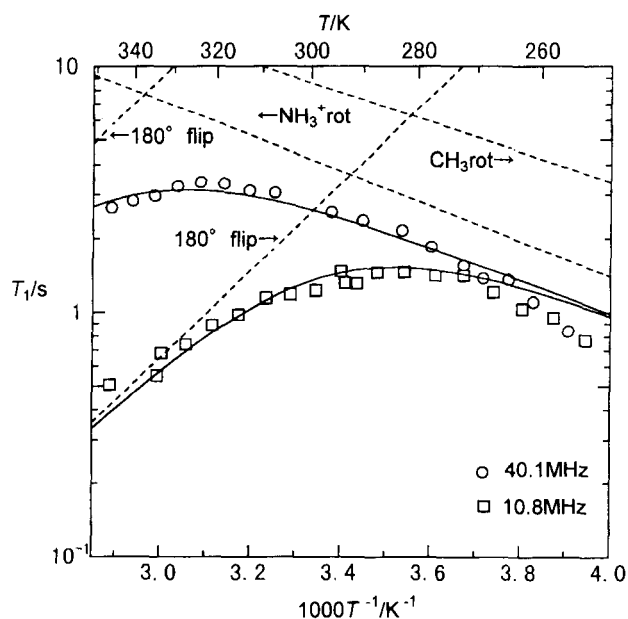


Fig. 2. Temperature dependences of ^1H NMR T_1 in phase II of $(n\text{-C}_5\text{H}_{12}\text{NH}_3)_2\text{ZnCl}_4$. Solid curves are the best-fitted calculated ones. Broken curves are contributions from respective molecular motions (see text).

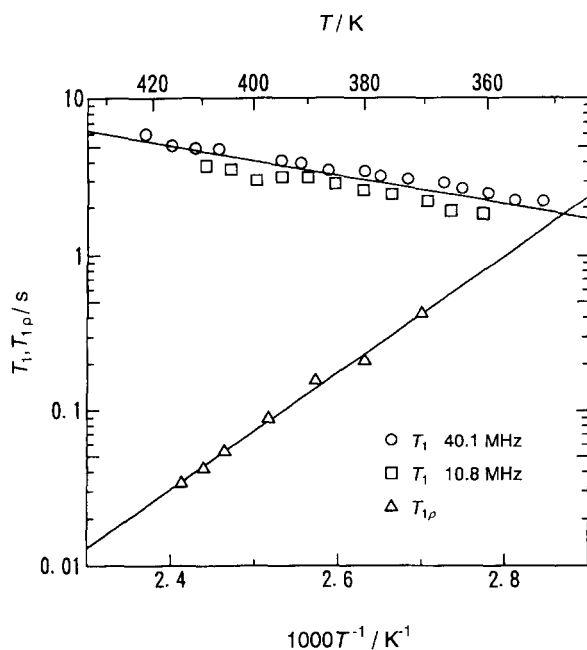


Fig. 3. Temperature dependences of ^1H NMR T_1 and $T_{1\rho}$ at an r.f. magnetic field of 3.97 G in phase I of $(n\text{-C}_5\text{H}_{12}\text{NH}_3)_2\text{ZnCl}_4$. Solid lines are the best-fitted calculated ones (see text).

their molecular axes; however, the axial rotation leads to the calculated M_2 value of ca. 8 G², which is much larger than the observed value. Hence, the rapid motion is dynamically more disordered than the uniaxial rotation and this disorder can be attributed to the orientational distribution of the cationic long axis about the crystallographic c -axis and/or the conformational disorder of the *trans-gauche* structure in

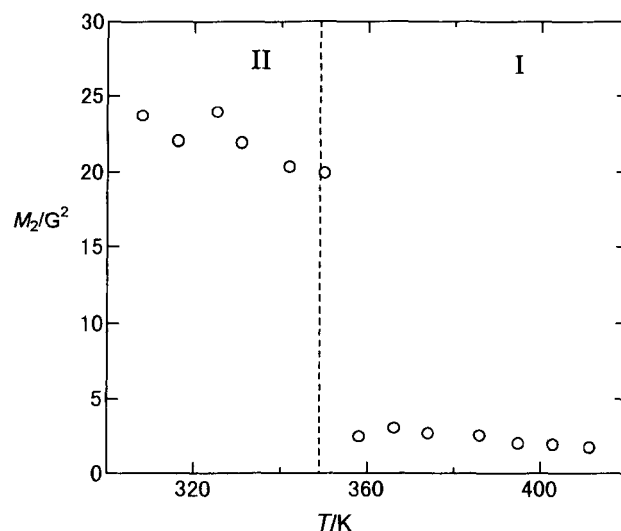


Fig. 4. A temperature dependence of M_2 of ^1H NMR linewidth in phases I and II of $(n\text{-C}_5\text{H}_{12}\text{NH}_3)_2\text{ZnCl}_4$. A broken line indicates the phase transition temperature of 349 K.

the alkyl chain. E_a of this composite motion was evaluated from the slope in the $\log T_1$ vs. T^{-1} plot, because in the fast motion limit of the BPP equation T_1^{-1} is proportional to τ_c . The resulting best fit line is represented in Fig. 3 and E_a of the motion was estimated to be 18 ± 2 kJ mol⁻¹.

The slow motion responsible for the temperature dependence of $T_{1\rho}$ was attributed to cationic translational self-diffusion. To confirm this, we measured the ac electrical conductivity σ between 340 and 420 K; this result is shown in Fig. 5. This clearly shows a marked ionic conduction in phase I. In general, the diffusion constant D for moving ions in crystals can be written by the following Nernst-Einstein

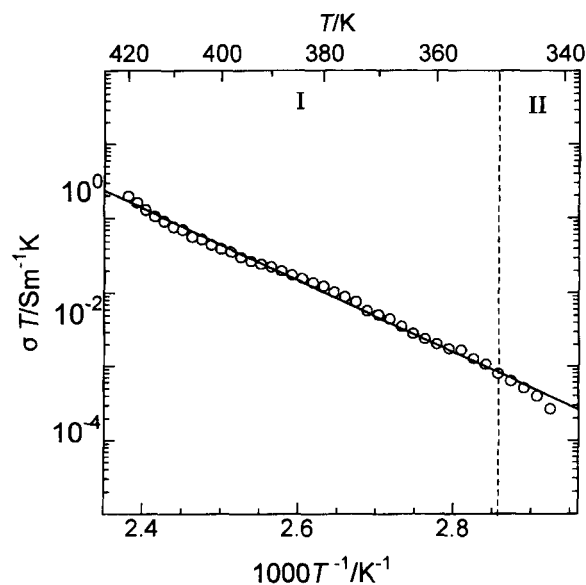


Fig. 5. A temperature dependence of ac electrical conductivity σ in phase I of $(n\text{-C}_5\text{H}_{12}\text{NH}_3)_2\text{ZnCl}_4$. A solid line is the best-fit Arrhenius relation given in text. A broken line denotes the phase transition temperature of 349 K.

equation:

$$D = \frac{kT\sigma}{(Ze)^2N}, \quad (2)$$

where Ze and N stand for the charge of the diffusing ion and the number of these ions in a unit volume, respectively. By assuming the Arrhenius relationship for the self-diffusion, D can be written as

$$D = D_0 \exp\left(-\frac{E_a}{RT}\right). \quad (3)$$

E_a determined from the slope in $\log(\sigma T)$ vs. T^{-1} plots was 85 ± 9 kJ mol $^{-1}$ and the obtained best fit line is depicted in Fig. 5. Since this compound has a layer structure, the ionic diffusion is most likely two-dimensional. If this is the case, $T_{1\rho}$ can no longer be expressed by the usual BPP-type equation. The temperature variation of $T_{1\rho}$ caused by 2D diffusion can be derived from the treatments by MacGillivray and Sholl,²⁵ who calculated the relaxation rates in a 2D square lattice. In the limit of slow diffusion and very low concentration of vacancies, the $T_{1\rho\text{diff}}$ equation approximately applicable to the present system is given by

$$T_{1\rho\text{diff}}^{-1} = \left(0.074545 \frac{8}{9} \frac{\gamma^4 \hbar^2 N C_V Z}{a^6 \omega_l^2}\right) \tau_c^{-1}, \quad (4)$$

where ω_l , N , C_V , Z , and a represent the Larmor frequency in the spin-locking r.f. magnetic field, the number of protons taking part in the diffusion, the concentration of lattice vacancies, the number of the nearest cationic sites for the diffusional jumps and the lattice constant corresponding to this jump. E_a of the slow motion was evaluated to be 72 ± 7 kJ mol $^{-1}$ from the slope in $\log T_{1\rho}^{-1}$ vs. T^{-1} plots using Eqs. 4 and 1. Two E_a values derived from $T_{1\rho}$ and σ are nearly the same, which confirms that the temperature variation of $T_{1\rho}$ can be ascribed to the cationic self-diffusion.

(*n*-C₁₂H₂₅NH₃)₂ZnCl₄. (*n*-C₁₂H₂₅NH₃)₂ZnCl₄ exhibited two heat anomalies, in good agreement with those in the previous report;¹⁵ one was attributed to a structural phase transition and the other to the fusion. The phases above and below the phase transition temperature of 362 K are named high-temperature phase (HTP) and room-temperature phase (RTP), respectively. An X-ray powder diffraction pattern taken at 292 ± 1 K in RTP was well explained by the reported monoclinic structure (space group $P2_1/c$).²⁶ An X-ray pattern at 389 ± 2 K in HTP with no structural data, showed only a few (00*l*) peaks.

¹H NMR T_1 was measured as a function of temperature at Larmor frequencies of 40.2, 25.5, and 12.8 MHz (89–415 K). The results are shown in Fig. 6. A discontinuity in T_1 was observed at 362 K, consistent with the thermal measurement. The asymmetric T_1 minimum observed in RTP was analyzed by the BPP equation;²¹ these results are shown in Fig. 6 and Table 2. We see that three thermal motions are effective in T_1 . By calculating M_2 values, the two shallow minima on the low-temperature side were assigned to the threefold reorientations of the two crystallographically non-equivalent CH₃ groups.

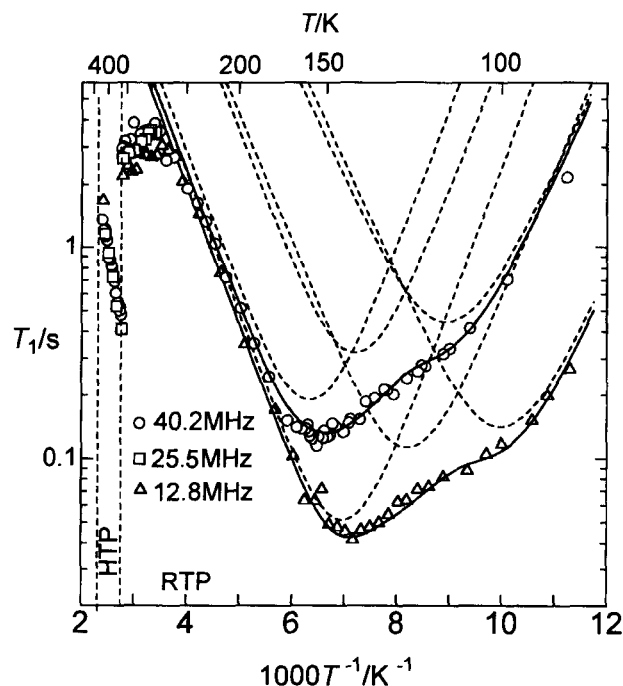


Fig. 6. Temperature dependences of ¹H NMR T_1 observed in (*n*-C₁₂H₂₅NH₃)₂ZnCl₄. Solid curves are the best-fitted calculated ones. Broken curves are contributions from respective molecular motions (see text). Vertical broken lines stand for the phase transition temperatures.

Table 2. Activation Energies, E_a , Pre-exponential Factors, τ_{c0} , and Motional Modes of *n*-Dodecylammonium Cations in (*n*-C₁₂H₂₅NH₃)₂ZnCl₄ Determined by ¹H NMR T_1 and $T_{1\rho}$

Phase	E_a	τ_{c0}	Motional mode
	kJ mol $^{-1}$	10 $^{-13}$ s	
RTP	8.8 ± 0.9	2.4 ± 0.2	CH ₃ rotation
	11 ± 0.1	2.3 ± 0.2	CH ₃ rotation
	13 ± 0.1	1.3 ± 0.1	NH ₃ ⁺ rotation
HTP	23 ± 2		Axial rotation + conformational disorder
	76 ± 8		Self-diffusion
	74 ± 7 ^{a)}		Self-diffusion

a) Derived from electrical conductivity.

In the high-temperature region of RTP, T_1 reached a maximum and became short on heating indicating that a new motion is excited just below the transition temperature. The temperature dependence of M_2 of ¹H NMR linewidth observed between 294 and 402 K is displayed in Fig. 7. A gradual decrease in M_2 over a wide temperature range upon heating observed in RTP can be attributed to molecular motions in a potential well with unequal minima.²⁷ With referring to the analysis in (*n*-C₅H₁₁NH₃)₂ZnCl₄, this motion can be assigned to the 180° flip of the entire cations about their molecular axes. Since the phase transition at 362 K is of order–disorder type, potential wells for this motion of entire cations are expected to have unequal minima in RTP.

The temperature variation of ¹H NMR $T_{1\rho}$ observed in

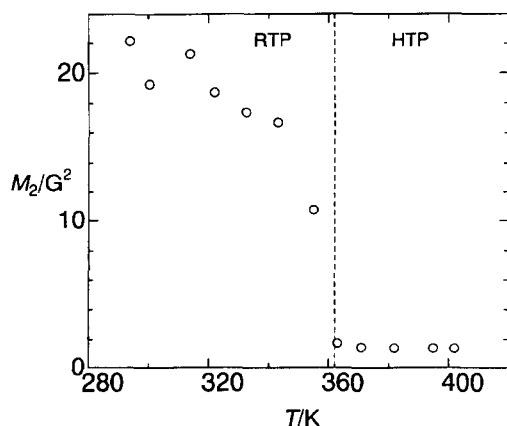


Fig. 7. A temperature dependence of M_2 of ^1H NMR linewidth observed in $(n\text{-C}_{12}\text{H}_{25}\text{NH}_3)_2\text{ZnCl}_4$. A broken line indicates the phase transition temperature of 362 K.

HTP is shown in Fig. 8 together with T_1 data. These results are quite similar to those obtained in phase I of $(n\text{-C}_5\text{H}_{11}\text{NH}_3)_2\text{ZnCl}_4$ given in Fig. 3, suggesting the superimposed motions. M_2 of ca. 1.5 G^2 observed in HTP is nearly the same as those observed in phase I of $(n\text{-C}_5\text{H}_{11}\text{NH}_3)_2\text{ZnCl}_4$ shown in Fig. 4. The temperature dependence of the ac electrical conductivity σ observed between 350 and 415 K is shown in Fig. 9. The results of the best fit to the data performed analogously to those in $(n\text{-C}_5\text{H}_{11}\text{NH}_3)_2\text{ZnCl}_4$ are given in Figs. 8 and 9 and Table 2. The temperature variation of T_1 was attributed to the uniaxial

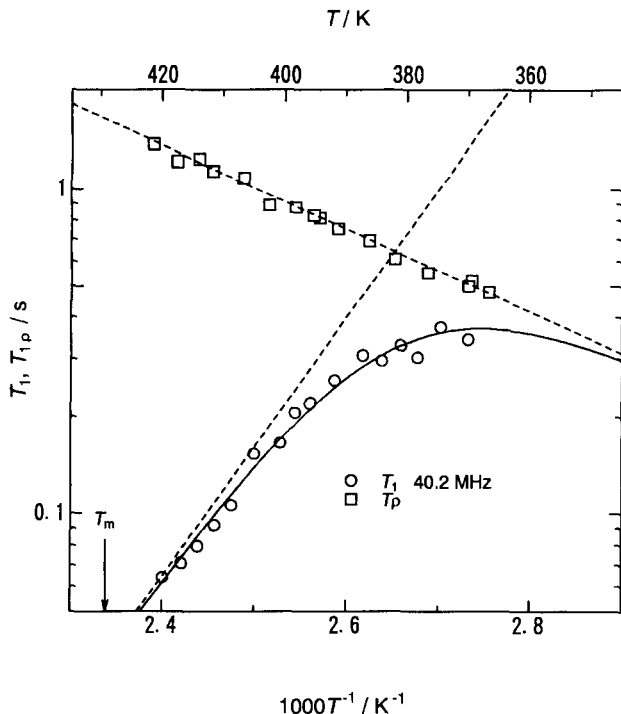


Fig. 8. Temperature dependences of ^1H NMR T_1 and $T_{1\rho}$ at an r.f. magnetic field of 3.97 G in HTP of $(n\text{-C}_{12}\text{H}_{25}\text{NH}_3)_2\text{ZnCl}_4$. A solid curve is the best-fitted calculated one. Broken lines are contributions from respective molecular motions (see text).

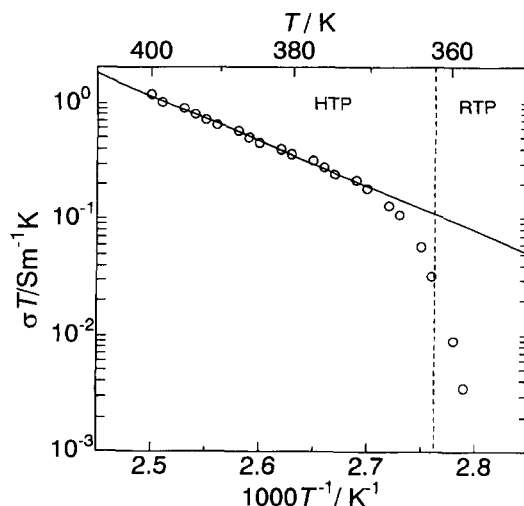


Fig. 9. A temperature dependence of a.c. electrical conductivity σ in HTP of $(n\text{-C}_{12}\text{H}_{25}\text{NH}_3)_2\text{ZnCl}_4$. A solid line is the best-fit Arrhenius relation given in text. A broken line represents the phase transition temperature of 362 K.

rotation of rigid cations about their molecular axes, accompanied by the orientational distribution of the axes and/or conformational disorder. The cationic self-diffusion is responsible for the temperature dependences of $T_{1\rho}$ and σ .

Discussion

Phase Transitions. Small transition entropies ΔS_t of 2— $3\text{ J K}^{-1}\text{ mol}^{-1}$ were observed at V–IV and IV–III transitions in $(n\text{-C}_5\text{H}_{11}\text{NH}_3)_2\text{ZnCl}_4$.^{13,20} In phase III, both of the crystallographically nonequivalent N atoms have five neighboring Cl atoms with N...Cl distances of 3.2—3.5 Å, suggesting disordered hydrogen bonds.¹⁰ Gomez Cuevas et al. suggested that these phase transitions could be related with the changes in the N–H...Cl hydrogen bonds scheme that lead to an ordered low-temperature phase.²⁰ If this is the case, the ordered phase has a potential well with unequal minima for NH_3^+ motion, and a discontinuous change in the potential energy curve occurs in the first-order transitions at 141.5 and 148 K. This should affect the temperature dependence of T_1 , as can be expected from our analysis shown in Fig. 1; however, we could not detect any anomaly in T_1 curve observed around transition temperatures and in phase V, suggesting that the NMR result contradicts the above picture.

Thermal and X-ray studies on the structural phase transition at 250 K in $(n\text{-C}_5\text{H}_{11}\text{NH}_3)_2\text{ZnCl}_4$ revealed the onset of an order-disorder transition for the orientation of the rigid pentylammonium chains which take two disordered sites about their molecular axes in phase II.¹⁰ This was confirmed by our analysis that the 180° flip of rigid cations about their molecular long axes is excited in phase II. From the present study, it is shown that this disorder is dynamical. Since the transition is first-order, the potential curve for the flip motion should be discontinuously altered at the transition. However, no discontinuity in T_1 was observed at the III–II transition; this is because, as can be seen from the analysis given in Fig. 2, T_1 around 250 K governed mostly by the NH_3^+ rotation masks

the 180° flip contribution.

Phase I in $(n\text{-C}_5\text{H}_{11}\text{NH}_3)_2\text{ZnCl}_4$ is believed to be in a conformationally highly disordered state.²⁰ This is consistent with our analysis that the chain conformations are dynamically disordered. These conformational defects seem to be kinks and end-*gauche*, because, if a successive *gauche* conformation were allowed, a wide space should be required in *ab*-plane of phase I; however, both *a*- and *b*-axes have nearly the same length in phase I and II. Since four consecutive C or N atoms are involved in the definition of a torsion angle, $n\text{-C}_5\text{H}_{11}\text{NH}_3^+$ chain has three independent possibilities to form either *trans* and *gauche* conformations. From the reported ΔS_t of $26 \text{ J K}^{-1} \text{ mol}^{-1}$,¹³ a conformational entropy per one C(or N)–C–C–C group is estimated to be $4.3 \text{ J K}^{-1} \text{ mol}^{-1}$ suggesting that each C(or N)–C–C–C group can be interpreted as an independent pseudospin with two equivalent sites. This means that a rotation about –C–C– is not free and chain conformations are not completely melted.

A very large ΔS_t of $133 \text{ J K}^{-1} \text{ mol}^{-1}$ was observed in $(n\text{-C}_{12}\text{H}_{25}\text{NH}_3)_2\text{ZnCl}_4$.¹⁵ This transition is characterized by both the order-disorder of rigid alkylammonium cations about their molecular axes and cooperative conformational changes in the alkyl chains.¹⁵ These results indicate that HTP in $(n\text{-C}_{12}\text{H}_{25}\text{NH}_3)_2\text{ZnCl}_4$ and phase I in $(n\text{-C}_5\text{H}_{11}\text{NH}_3)_2\text{ZnCl}_4$ are quite similar in dynamical state of cations. There are, however, some differences between the two phases: the X-ray powder diffraction pattern taken in $(n\text{-C}_{12}\text{H}_{25}\text{NH}_3)_2\text{ZnCl}_4$ showed only a few (00*l*) peaks, while that for $(n\text{-C}_5\text{H}_{11}\text{NH}_3)_2\text{ZnCl}_4$ showed some more peaks; a melting entropy ΔS_m of $(n\text{-C}_5\text{H}_{11}\text{NH}_3)_2\text{ZnCl}_4$ was $33 \text{ J K}^{-1} \text{ mol}^{-1}$,¹³ while that of $(n\text{-C}_{12}\text{H}_{25}\text{NH}_3)_2\text{ZnCl}_4$ was $17 \text{ J K}^{-1} \text{ mol}^{-1}$.¹⁵ These results show that HTP is more disordered than phase I. The positional order of both cations and anions seems to remain in both phases, judging from the X-ray powder patterns taken in phase I and HTP, suggesting that there are periodic arrangements in crystals. Moreover, the present NMR results suggest that the orientational and conformational order of the cations in phase I and HTP are almost the same. Accordingly, it is highly possible that the difference between phase I and HTP is caused by the orientational order of ZnCl_4^{2-} . In our previous study on $(n\text{-C}_n\text{H}_{2n+1}\text{NH}_3)_2\text{ZnCl}_4$ compounds,¹³ we have estimated the contributions from the orientational order of the anions to ΔS_m to be $17 \text{ J K}^{-1} \text{ mol}^{-1}$. Using these results, we see that the orientational order of rigid anions is almost lost in HTP but conserved in phase I, and hence we can conclude that the phase transition at 362 K in $(n\text{-C}_{12}\text{H}_{25}\text{NH}_3)_2\text{ZnCl}_4$ is accompanied by orientational disordering of cations about their molecular axes and of anions as a whole, and by the cooperative conformational melting of alkylammonium chains. From the observed ΔS_t of $133 \text{ J K}^{-1} \text{ mol}^{-1}$, contributions from the orientational disorders of cations and anions should be subtracted for estimating only the conformational contribution to ΔS_t . Since a hindered rotation of cations about one axis has contribution of *R* to entropy and since the orientational entropy of ZnCl_4 is estimated to be $17 \text{ J K}^{-1} \text{ mol}^{-1}$, the conformational contribution is evaluated to be about

$100 \text{ J K}^{-1} \text{ mol}^{-1}$. Accordingly, the conformational entropy per one C(or N)–C–C–C group becomes approximately $5 \text{ J K}^{-1} \text{ mol}^{-1}$, suggesting disordering between two sites. The conformational defects, the majority of which seem to be kinks, move along the chain axis, so that chains are regarded to be melted. The chains are, however, not completely melted in HTP and some orders in chain conformations remain partly even in a liquid phase, at least just above the melting point.

Molecular Dynamics. From the present experimental results, it follows that phase I in $(n\text{-C}_5\text{H}_{11}\text{NH}_3)_2\text{ZnCl}_4$ and HTP in $(n\text{-C}_{12}\text{H}_{25}\text{NH}_3)_2\text{ZnCl}_4$ are the rotator phases, because the following motions characteristic in the rotator phase were observed. Namely, the uniaxial rotation accompanied by diffusion of conformational intrachain defects along the chain axis and two-dimensional cationic self-diffusion take place. On the other hand, we notice some differences in rotator phases of $(n\text{-C}_n\text{H}_{2n+1}\text{NH}_3)_2\text{ZnCl}_4$ and *n*-alkylammonium chlorides (abbreviated to C_nCl).^{2–6} The temperature ranges of the rotator phases in $(n\text{-C}_5\text{H}_{11}\text{NH}_3)_2\text{ZnCl}_4$ and $(n\text{-C}_{12}\text{H}_{25}\text{NH}_3)_2\text{ZnCl}_4$ are 350–436 K and 362–438 K, respectively, narrower than those in C_nCl (C_5Cl : 256–503 K; C_{12}Cl : 345–475 K). In the ^1H NMR relaxation due to the cationic uniaxial reorientation, the non-linear $\log T_1$ vs. T^{-1} curve has been observed in C_nCl except for C_{12}Cl ; however, $\log T_1$ vs. T^{-1} plots were linear in $(n\text{-C}_5\text{H}_{11}\text{NH}_3)_2\text{ZnCl}_4$ and $(n\text{-C}_{12}\text{H}_{25}\text{NH}_3)_2\text{ZnCl}_4$. The self-diffusion of the anions was not observed in phase I and HTP, while it was activated in C_nCl . E_a values of the cationic self-diffusion in $(n\text{-C}_5\text{H}_{11}\text{NH}_3)_2\text{ZnCl}_4$ and $(n\text{-C}_{12}\text{H}_{25}\text{NH}_3)_2\text{ZnCl}_4$ are nearly the same, while those in C_nCl depend on the length of the carbon chain. We need some more systematic experiments on $(n\text{-C}_n\text{H}_{2n+1}\text{NH}_3)_2\text{ZnCl}_4$ to conclude that these differences are generally observed between $(n\text{-C}_n\text{H}_{2n+1}\text{NH}_3)_2\text{ZnCl}_4$ and C_nCl . In what follows we discuss only the translational self-diffusion of alkylammonium ions.

It was reported that $(n\text{-C}_5\text{H}_{11}\text{NH}_3)_2\text{ZnCl}_4$ forms an orthorhombic lattice in phase I;²⁰ however, detailed structural data in phase I and HTP are unavailable. According to Refs. 10 and 20, the crystal structure of phase II is orthorhombic with space group *Pnma* and $a = 10.323$, $b = 7.406$, and $c = 25.171 \text{ Å}$ at 295 K; the cell parameters for phase I are: $a = 10.2$, $b = 7.1$, and $c = 27.9 \text{ Å}$ at 349 K. We see that the lengths of *a*- and *b*-axes are nearly the same in both phases, while *c*-axis in phase I increases by approximately 11%. This drastic change in *c*-axis at the transition can be interpreted as follows.²⁰ The all-*trans* and intercalated carbon chains in phase II transform to the non-intercalated chains that have shorter length and larger diameter due to kink and end-*gauche* structures in phase I, as is schematically depicted in Fig. 10. A phase transition from an intercalated to a non-intercalated bilayer structure was first reported in C_{10}Cl , which is reconstructive and not reversible.²⁸ The I–II and HTP–RTP transitions are however reversible. Such a cell expansion at a phase transition from the second highest-temperature to the highest-temperature phase was observed in $(n\text{-C}_{13}\text{H}_{27}\text{NH}_3)_2\text{ZnCl}_4$ and $(n\text{-C}_{14}\text{H}_{29}\text{NH}_3)_2\text{ZnCl}_4$ with 19²⁹ and 17.5%³⁰ increase in *c*-axis, respectively. Moreover, our

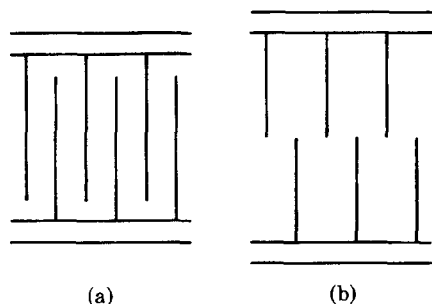


Fig. 10. The schematic representation of (a) intercalated and (b) non-intercalated layer structures.

X-ray powder diffraction gave $c = 51.7 \text{ \AA}$ in HTP increased by 16.4%. Since it is clear that a non-intercalated structure is preferable for a diffusion of alkylammonium chains and in fact phase I and HTP showed a relatively high ionic conductivity of ca. $10^{-3} \Omega^{-1} \text{ m}^{-1}$ comparable to that in $C_n\text{Cl}$, it is most likely that phase I and HTP have the non-intercalated structure.

The ionic conductivities in phase I and HTP are expected to be anisotropic due to their layer structures. That is, the self-diffusion constant within the layer, D_{\perp} , is thought to be different from that along the c -axis, D_{\parallel} . In the present case, D_{\perp} can be approximately related to the correlation time of the motion, τ_D , by the equation

$$D_{\perp} = \frac{d^2}{4\tau_D}, \quad (5)$$

where, d is the nearest jump distance. Assuming that ions jump to the nearest Schottky-type lattice defects, d in phase I can be estimated to be 6.0 and 6.7 \AA based on the crystal structural data in phase II, because a - and b -lengths scarcely change at I–II transition. Since RTP has $a = 7.409$ and $b = 10.379 \text{ \AA}$ and it is expected that HTP has nearly the same a - and b -lengths as in RTP,²⁶ d in HTP is also estimated to be 6–7 \AA . These values are somewhat longer than 5.0–5.2 \AA reported for $C_n\text{Cl}$.^{2–5} Using Eq. 5, we evaluated τ_D . Here the diffusional correlation time extrapolated to the melting point, $\tau_D(T_m)$, was calculated using $d = 6.4 \text{ \AA}$, leading to the order of 10^{-7} s for phase I and HTP. It has been reported that the same order of $\tau_D(T_m)$ is observed independent of compounds and melting points for plastic crystals and rotator phases in $C_n\text{Cl}$.⁵

The activation energies of cationic self-diffusion, E_a , in phase I in $(n\text{-C}_5\text{H}_{11}\text{NH}_3)_2\text{ZnCl}_4$ and HTP in $(n\text{-C}_{12}\text{H}_{25}\text{NH}_3)_2\text{ZnCl}_4$ have similar values of 70–80 kJ mol^{-1} , while those of rotator phases in $C_n\text{Cl}$ depend on the chain length, i.e., E_a increases with increasing the chain length (C_5Cl : 50 kJ mol^{-1} ; C_{12}Cl : 100 kJ mol^{-1}). This suggests that inter-chain interactions, i.e., van der Waals force, are very effective to the potential barrier for the diffusion in $C_n\text{Cl}$. At least in C_{12}Cl , the interactions are seems to be dominant. The inter-chain interactions, however, seem to be less effective in $(n\text{-C}_n\text{H}_{2n+1}\text{NH}_3)_2\text{ZnCl}_4$, because their inter-chain distances are longer than those in $C_n\text{Cl}$. Hence, it is expected that anion–cation interactions, mainly $\text{N-H}\cdots\text{Cl}$

hydrogen bonds, are more important in the potential energy for the diffusion in $(n\text{-C}_n\text{H}_{2n+1}\text{NH}_3)_2\text{ZnCl}_4$. As described previously, an orientational order of anions is preserved in phase I but is lost in HTP. It appears that this can also affect E_a of the diffusion, i.e., the disorder of anions can weaken the hydrogen bonds. Accordingly, it is concluded that the anion–cation interactions are more effective than inter-chain interactions especially in phase I and the orientational disordering of anions in HTP makes the barrier lower.

Conclusion

Phase I in $(n\text{-C}_5\text{H}_{11}\text{NH}_3)_2\text{ZnCl}_4$ and HTP in $(n\text{-C}_{12}\text{H}_{25}\text{NH}_3)_2\text{ZnCl}_4$ were found to be rotator phases where two distinct motions are excited. One is the uniaxial rotation of alkylammonium cations about their molecular long axes, accompanied by the conformational disorder in the chains such as kinks. Phase I and HTP are believed to be in such a high conformational disordered state that chains can be regarded as melting. The organic chains are however not completely melted and some orders in conformations remain, i.e., rotations about C–C axes are not free but reorientational jumps with two equivalent sites.

The other motion is the two-dimensional self-diffusion of the cations moving within the layer perpendicular to the c -axis. It is most likely that the alkyl chains are non-intercalated in phase I and HTP, so that the cationic diffusion is expected to be easily excited with the diffusional correlation time of the order of 10^{-7} s extrapolated to the melting point. The same order values were observed at the melting temperatures in plastic crystals and $C_n\text{Cl}$ compounds. $\text{N-H}\cdots\text{Cl}$ hydrogen bonds affect the diffusional activation energy more than inter-chain interactions, which are important in $C_n\text{Cl}$ compounds. It can be concluded that the rotator phases newly found here are quite analogous to those detected in $C_n\text{Cl}$ compounds, although there are some differences.

In a temperature range between ca. 120 K and the melting point, $(n\text{-C}_5\text{H}_{11}\text{NH}_3)_2\text{ZnCl}_4$ shows four first-order structural phase transitions; however, $(n\text{-C}_{12}\text{H}_{25}\text{NH}_3)_2\text{ZnCl}_4$ undergoes only a single transition. All of these transitions are regarded as order–disorder type. The I–II, II–III, and RTP–HTP transitions are related with disordering of alkylammonium ions. The II–III transition is an order–disorder one of the rigid pentylammonium ions with two equivalent sites about their molecular axes. In the I–II transition, the orientational order of cations about the axes is completely lost and a conformational melting takes place. The RTP–HTP transition can correspond to that between phase III and I in $(n\text{-C}_5\text{H}_{11}\text{NH}_3)_2\text{ZnCl}_4$, with a difference that the orientational order of ZnCl_4^{2-} ions is lost in HTP but preserved in phase I.

This work was partly supported by a Grant-in-Aid for Scientific Research No. (B) 09440234 from the Ministry of Education, Science, Sports and Culture.

References

- 1 A. Mueller, *Proc. R. Soc. London, Ser. A*, **138**, 514 (1932).
- 2 S. Fukada, H. Yamamoto, R. Ikeda, and D. Nakamura, *J. Chem. Soc., Faraday Trans. 1*, **83**, 3207 (1987).
- 3 M. Hattori, S. Fukada, D. Nakamura, and R. Ikeda, *J. Chem. Soc., Faraday Trans.*, **86**, 3777 (1990).
- 4 S. Iwai, R. Ikeda, and D. Nakamura, *Can. J. Chem.*, **66**, 1961 (1988).
- 5 S. Iwai, M. Hattori, D. Nakamura, and R. Ikeda, *J. Chem. Soc., Faraday Trans.*, **89**, 827 (1993).
- 6 S. Tanaka, N. Onoda-Yamamoto, S. Ishimaru, and R. Ikeda, *Bull. Chem. Soc. Jpn.*, **70**, 2981 (1997).
- 7 J. Timmermans, *J. Phys. Chem. Solids*, **18**, 1 (1961).
- 8 T. Shimizu, S. Tanaka, N. Onoda-Yamamoto, S. Ishimaru, and R. Ikeda, *J. Chem. Soc., Faraday Trans.*, **93**, 321 (1997).
- 9 F. J. Zuniga, M. J. Tello, J. M. Perez-Mato, M. A. Perez-Jubindo, and G. Chapuis, *J. Chem. Phys.*, **76**, 2610 (1982).
- 10 A. Gomez-Cuevas, M. J. Perez-Mato, M. J. Tello, G. Masariaga, J. Fernandez, A. Lopez-Echarri, F. J. Zuniga, and G. Chapuis, *Phys. Rev. B*, **B29**, 2655 (1984).
- 11 K. Horiuchi, *J. Phys. Soc. Jpn.*, **63**, 363 (1994).
- 12 K. Horiuchi and A. Weiss, *J. Mol. Struct.*, **345**, 97 (1995).
- 13 Y. Sakiyama, K. Horiuchi, and R. Ikeda, *J. Phys.: Condens. Matter*, **8**, 5345 (1996).
- 14 H. Ishihara, S.-q. Dou, K. Horiuchi, H. Paulus, H. Fuess, and A. Weiss, *Z. Naturforsch., A*, **52a**, 550 (1997).
- 15 C. Socias, M. A. Arriandiaga, M. J. Tello, L. Fernandez, and P. Gili, *Phys. Stat. Sol.(A)*, **57**, 405 (1980).
- 16 Y. Kume, R. Ikeda, and D. Nakamura, *J. Magn. Reson.*, **33**, 331 (1979).
- 17 T. Kobayashi, H. Ohki, and R. Ikeda, *Mol. Cryst. Liq. Cryst.*, **257**, 279 (1994).
- 18 D. C. Look and I. J. Lowe, *J. Chem. Phys.*, **44**, 2995 (1966).
- 19 J. G. Powles and J. H. Strange, *Proc. Phys. Soc.*, **82**, 6 (1963).
- 20 A. Gomez Cuevas, M. J. Tell, and A. Lopez Echarri, *J. Phys. Chem. Solids*, **45**, 1175 (1984).
- 21 N. Bloembergen, E. M. Purcell, and R. V. Pound, *Phys. Rev.*, **73**, 679 (1948).
- 22 J. H. Van Vleck, *Phys. Rev.*, **74**, 1168 (1948).
- 23 S. Fukada, R. Ikeda, and D. Nakamura, *Bull. Chem. Soc. Jpn.*, **57**, 2802 (1984).
- 24 S. Fukada, R. Ikeda, and D. Nakamura, *Z. Naturforsch., A*, **40a**, 347 (1984).
- 25 I. R. MacGillivray and C. A. Sholl, *J. Phys. C*, **18**, 1691 (1985).
- 26 M. R. Ciajolo, P. Corradini, and V. Pavone, *Acta Crystallogr., Sect. B*, **B33**, 553 (1977).
- 27 Y. Ito, T. Asaji, R. Ikeda, and D. Nakamura, *Ber. Bunsenges. Phys. Chem.*, **92**, 885 (1988).
- 28 R. Kind, R. Blinc, H. Arend, P. Muralt, J. Slak, G. Chapuis, K. J. Schenk, and B. Zeks, *Phys. Rev. A*, **A26**, 1816 (1982).
- 29 F. J. Zuniga and G. Chapuis, *Mol. Cryst. Liq. Cryst.*, **128**, 349 (1985).
- 30 J. Fernandez, C. Socias, M. A. Arriandiaga, M. J. Tello, and A. Lopez Echarri, *J. Phys. C: Solid State Phys.*, **15**, 1151 (1982).